9th AIAA/ASME Joint Thermophysics and Heat Transfer Conference
5 - 8 June 2006, San Francisco, California

AIAA 2006-3116

Energy Coupling Through the Small Gap in Optical Microcavities

Haiyong Quan* and Zhixiong Guo†
Rutgers, The State University of New Jersey, Piscataway, NJ, 08854

In this report, we investigate the influences of the small gap in whispering-gallery modes on energy coupling, resonance quality and frequency. Photon tunneling between an optical resonator and its light-delivery coupler depends strongly on the gap dimension which can vary from zero to size of an optical wavelength involved. An optimal gap dimension is found to exist for maximum energy coupling. The *Q* factor increases exponentially with increasing gap and saturates as the gap approaches the optical wavelength. The resonance frequency shifts with decreasing gap to a certain value. An optimum gap for sensing applications can be defined at the half maximum energy coupling where both the *Q* factor and coupling efficiency are high and the resonance frequency is little affected by the gap variation.

Nomenclature

c	=	speed of light
d	=	diameter of microcavity
$\overline{e}$	=	direction unit vector
$\overline{E}$	=	electric field vector
g	=	gap distance
$\overline{H}$	=	magnetic field vector
$\overline{J}$	=	electric current density
k	=	absorption index
m	=	complex index of refraction
n	=	real part of the refractive index
$\overline{n}$	=	unit vector in normal direction
Q	=	cavity quality factor
ε	=	permittivity
ε_c	=	complex permittivity
λ	=	wavelength
μ	=	permeability
ρ	=	electric charge density
σ	=	electrical conductivity
ω	=	angular frequency
$\Delta\omega$	=	resonance bandwidth

I. Introduction

Optical microcavities[1] have recently received increasing attention due to their high potential for the realization of cavity quantum electrodynamics,[2] microlasers,[3] narrow filters,[4] optical switching,[5] miniature biosensors,[6] and high resolution spectroscopy,[7] to name but a few. Whispering-gallery mode resonances occur when light travels in a dielectric medium of circular geometry. After repeated total internal reflections (TIR) at the curvilinear boundary the electromagnetic wave returns to its starting point in phase, giving rise to resonance. If the resonating cavity is in the micrometer level, one obtains a very small mode volume and high finesse.

* Graduate Student, Department of Mechanical and Aerospace Engineering, 98 Brett Road.
† Assistant Professor, Department of Mechanical and Aerospace Engineering, 98 Brett Road.

Despite of very small volume, WGM optical microcavities can store high energy due to the minimum reflection losses inside the cavity. The resonant quality is described by the cavity Q factor that is defined as 2π times the ratio of the stored energy in the microcavity to its energy lost per optical period. $Q > 10^9$ has been observed at red and near-infrared wavelengths in fused-silica sub-millimeter particles.[8,9] If used as miniature sensors optical microcavities could achieve extremely high sensitivity for detection of molecules such as proteins[6] and peptides.[10]

Finesse is defined as a ratio of free-spectral range (FSR) to full-width at half maximum (FWHM) of a resonant band. FSR represents the interval between two adjacent resonant frequencies and is inversely proportional to the cavity size. Microscale cavities ensure that the resonant frequencies are more sparsely distributed throughout the cavity size-dependent resonant optical spectrum than they are in corresponding mesoscale cavities. However, it should be aware of that the effects of diffraction grow as the cavity shrinks; and when the periphery of the cavity approaches the wavelength of light passing through the interior, resonances are lost altogether.

Different from Mie resonance in microdroplets of aerosols which is observable by means of elastic and inelastic scattering of free-space beams, high-Q WGMs are not accessible by free-space beams; and therefore, require employment of near-field couplers. Numerous coupling devices, such as high-index prisms with frustrated total internal reflection,[11] side-polished fiber couplers,[12] tapered optical fibres tapers,[13] and waveguides,[14] have been considered. The principle of all these devices is based on providing efficient energy transfer to the resonant circular TIR guided wave in the resonator through the evanescent field of a guided wave or a TIR spot in the coupler. It is evident *a priori* that efficient coupling can be expected on fulfillment of two main conditions: phase synchronism and significant overlap of the two evanescent fields in the gap between the microcavity and the coupler. Thus, the gap is a critical parameter that affects the energy transfer and coupling efficiency.

It is tough to control the gap for a lab-built optical microcavity. Recent advances in the technology of nanofabrication offer the possibility of manufacturing new optical devices with unprecedented control. It is now feasible to consider optical microcavities, light couplers, and coupling gaps having physical dimensions in nano- and micro-meter levels. Integration of photonic devices can be easily achieved through fabrication methods like optical lithography, chemical vapor deposition, and chemical or plasma etching. Dimensions of 100-200 nm are routinely achieved in the manufacturing of integrated circuits. Nanofabrication techniques allow the realization of semiconductor microcavity ring and disk resonators with evanescent wave coupling to micron- or submicron-width waveguides across nanoscale air gaps. With high-quality etching, the scattering loss can be minimized to achieve simultaneously a high Q and high finesse. For example, Guo et al.[15] recently nanofabricated integrated microcavities and waveguides using 248nm optical lithography and conventional silicon IC processing.

Radiative energy transfer, which involves photon transport and Maxwell electromagnetic interaction with matter, is an important heat transfer mechanism. Maxwell electromagnetism[16,17] is commonly used to describe radiation phenomena in micro/nanometer scale. Conventional thermal radiation transfer in meso/macroscale is well summarized in the textbooks.[18,19] Some specific criteria have been established to delineate the micro/nanoscale and the meso/macroscale radiation regimes.[20,21] The increasing demand for smaller structures and devices opens up new opportunities and challenges in micro/nanoscale heat transfer.[22-25]

In this study, we will characterize the micro/nanoscale energy transfer and optical resonance in optical microcavity devices. Each device consists of a resonant microcavity and a light-delivery waveguide coupled by a nano- to sub-microscale air gap. Maxwell's equations governing the energy transfer will be solved via the finite element method. Simulation results will be utilized to discuss the characteristics of energy coupling and storage capacity, and resonance quality and frequency in such kinds of devices.

II. Mathematical Description

The time-dependent Maxwell's equations are[16]

$$\begin{cases} \nabla\cdot\bar{E}=\dfrac{\rho}{\varepsilon}; \quad \nabla\times\bar{E}=-\mu\dfrac{\partial\bar{H}}{\partial t} \\ \nabla\cdot\bar{H}=0; \quad \nabla\times\bar{H}=\bar{J}+\varepsilon\dfrac{\partial\bar{E}}{\partial t} \end{cases} . \tag{1}$$

For the electric field, since $\rho = 0$ and $\bar{J} = \sigma\bar{E}$, we can derive the equation for $\bar{E}$ as follows:

$$\nabla^2\bar{E} - \mu\sigma\frac{\partial\bar{E}}{\partial t} - \mu\varepsilon\frac{\partial^2\bar{E}}{\partial t^2} = 0 . \tag{2}$$

For time-harmonic waves, $\bar{E}(\bar{r},t) = \bar{E}'(\bar{r})e^{i\omega t}$; Eq. (2) is then simplified to a Helmholtz equation:

$$\frac{1}{\mu}\nabla^2\overline{E} + \omega^2\varepsilon_c\overline{E} = 0, \tag{3}$$

where we have introduced the complex permittivity[19] $\varepsilon_c = \varepsilon_{cr}\cdot\varepsilon_0 = \varepsilon - i(\sigma/\omega)$, and $\varepsilon_{cr} = m^2 = n^2 - k^2 - i2nk$. We can get a similar Helmholtz equation for the magnetic field.

Under optical resonances the EM field inside the microcavity is typically consisted of equatorial brilliant rings. And the rings are located on the same plane as the waveguide. Further, the considered structure of nanofabricated microcavities is planar. So it is feasible to use a two-dimensional theoretical model. In the present calculations we consider the In-plane TE waves, where the electric field has only a *z*-component; and it propagates in the *x*-*y* plane. Thus, the fields can be written as:

$$\overline{E}(x,y,t) = E_z(x,y)\overline{e}_z e^{i\omega t},\ \overline{H}(x,y,t) = \left[H_x(x,y)\overline{e}_x + H_y(x,y)\overline{e}_y\right]e^{i\omega t}. \tag{4}$$

At the interface and physical boundaries, the natural continuity condition is used. For the boundaries of the calculation domain, the low-reflecting boundary condition is adopted. The low-reflecting condition means that only a small part of the wave is reflected, and that the wave propagates through the boundary almost as if it were not present. This condition can be formulized as

$$\overline{e}_z\cdot\overline{n}\times\sqrt{\mu}\overline{H} + \sqrt{\varepsilon}E_z = 0. \tag{5}$$

The light source term E_{0z}, which propagates inwards through the entry of the waveguide, was treated as an electrically low-reflecting boundary expressed by

$$\overline{e}_z\cdot\overline{n}\times\sqrt{\mu}\overline{H} + \sqrt{\varepsilon}E_z = 2\sqrt{\varepsilon}E_{0z}. \tag{6}$$

The quality factor *Q* is expressed by:

$$Q = \omega_0/\Delta\omega, \tag{7}$$

where ω_0 is the central frequency of a resonant band, and $\Delta\omega$ is the resonance bandwidth.

Versatile and accurate numerical approaches including the finite-difference time-domain method[26] and the finite element method[27] (FEM) can be employed for solving the above mathematical models. The FEM is more flexible in terms of the treatment of irregular configurations. Thus, the In-plane TE waves application mode of the commercial FEMLAB package (version 3.0) was employed for the finite element analysis in the current calculations. The description of the numerical method is available in a recent publication[10] of us.

III. Results and Discussion

We consider an optical microresonance systems consisting of a microdisk (as the resonator) and a coupling waveguide as shown in Fig. 1. The diameter of the microcavity is 2μm, and the width of the waveguide is 0.5μm. The microdisk and waveguide are made of the same material (silicon nitride) and are assumed to have a constant refractive index of 2.01. The resonance mode is around 823 nm wavelength. The surrounding medium is air. The gap is defined as the narrowest distance between a microdisk and its coupled waveguide. The gap varies from zero (in close contact) to one wavelength of incident radiation.

The simulation domain is meshed with many triangle elements generated automatically by the FEMLAB software in which a mesh gradient approach is adopted to deal with abrupt changes in sensitive areas like the vicinity around the periphery of the microdisk and the gap region. However, such an automatic approach was not very satisfactory because there is no constant gradient change in the resonant EM field existed inside the periphery of the cavity. To meet with this requirement, we divide the microdisk into two regions and use hierarchical meshing to scale the cavity down to two different spatial levels: a ring where resonant EM field exists and an inner disk where the EM field is very weak. The mesh in the ring is then locally refined. After such a treatment, the simulation was satisfactory. The total finite elements used were about 10^5. The computation was conducted in a PC. The CPU time consumption was basically not a

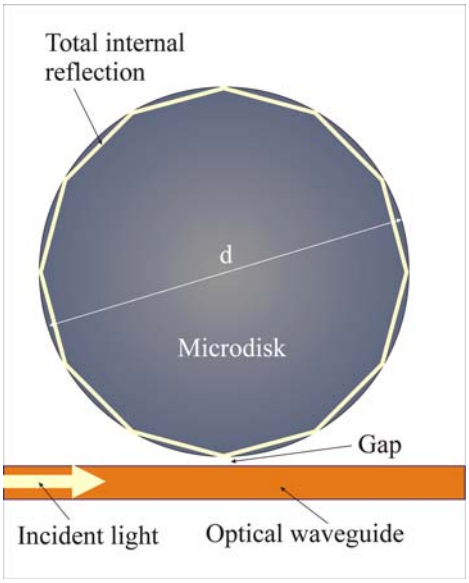

Figure 1. Schematic sketch of an optical microcavity system.

concern for an individual simulation run because each run only took several minutes. In order to get a resonance spectrum, however, hundreds of simulation runs are needed. In particular, the resonance band is extremely fine for larger gaps due to the high-*Q* characteristic of WGM microresonances. It takes dozens of runs to find a resonance band for each gap value in the WGM systems. The whole simulation can be very time-consuming.

Figure 2 shows the electric fields of the microcavity system for three different gap values. It is seen that the E-field in the cavity with 150nm gap is much stronger than those with 50nm and 400nm gap values. Since the energy density is proportional to the square of the amplitude of the time-harmonic E-field, the energy density in the cavity with 150nm gap is very concentrated. Thus, the gap dimension will absolutely affect the energy coupling from the waveguide to the microcavity. When the gap is very small (such as g = 50 nm), the E-field in the waveguide is distorted. While in the case of g = 400nm, the presence of the microcavity does not affect the E-field pattern in the waveguide.

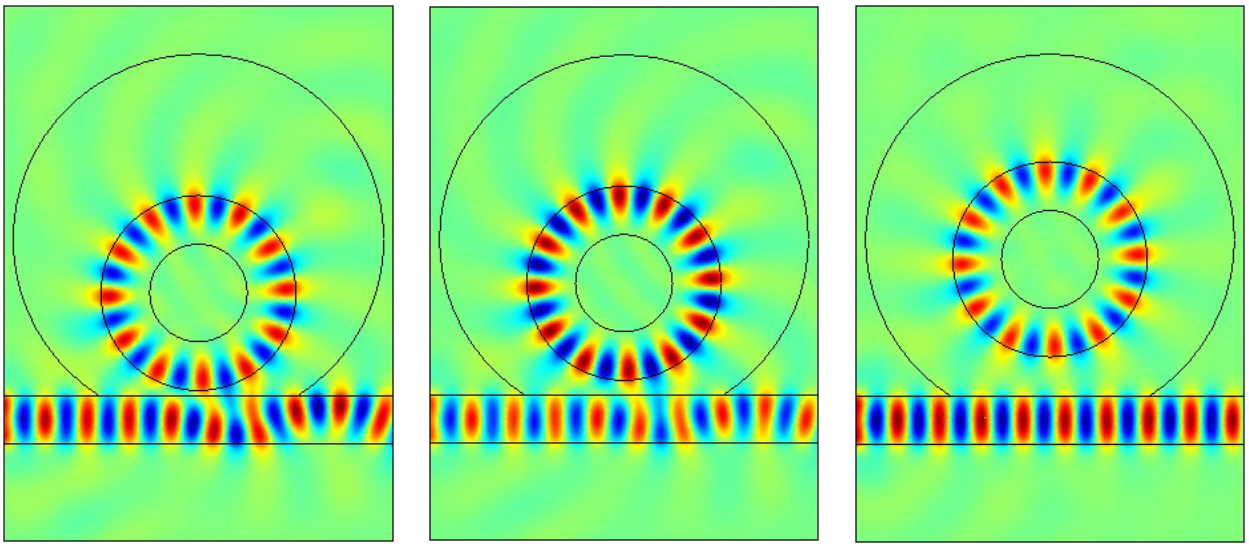

(a) g = 50nm (b) g = 150nm (c) g = 400nm

Figure 2. Electric fields of the system with three different gap values.

In Fig. 3, the stored energy inside the cavity is used as a measure to demonstrate the gap effect on energy coupling. The larger the stored energy, the stronger the energy transfer from the waveguide to the cavity; and consequently the more efficient in energy coupling. The simulated results are represented by the discrete symbols in Fig. 3. The results are fitted into Lorentz fittings. The results are normalized by the maximum stored energy at the optimal gap dimension. The gap varies from zero to 800nm with a step change of 50nm. It is estimated from the fitted curves that the energy storage is the greatest when the gap is about 180nm for the resonance mode at 823nm wavelength. Such an optimal gap value represents the most efficient energy coupling at the microcavity resonance mode. Thus, an optimal gap dimension does exist. This is of practical importance for microcavity device design. In

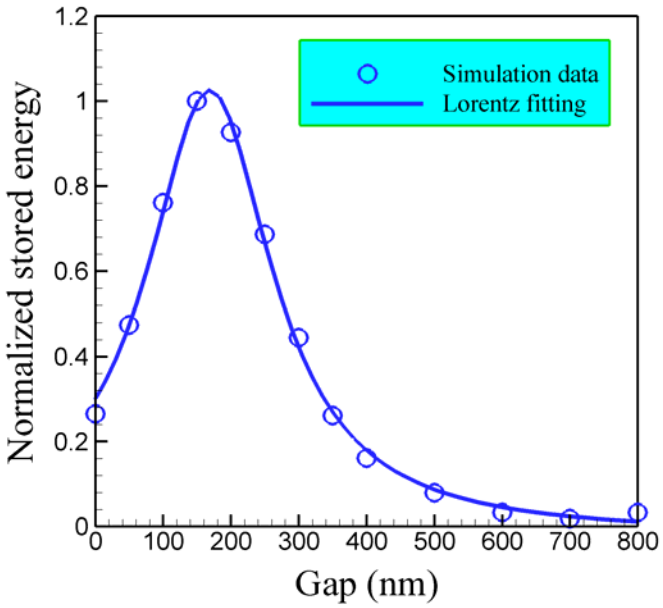

Figure 3. The stored energy in the microcavity vs. the gap variation.

particular, signal intensity is very important in sensor applications. One would like to design a gap with more efficient energy coupling.

The gap effect on resonance quality is shown in Fig. 4, where both the FWHM and *Q* factor are considered. The discrete symbols represent the simulated results and the variations can be fitted into Boltzmann fittings. We found that with the increasing gap from zero to 900nm, the FWHM (unit: GHz) narrows and the *Q* factor increases. The fitted curves show that the *Q* factor increases exponentially at the beginning before the gap reaches to the optimal gap for coupling; after passing the optimal gap, the increase of the *Q* factor slows down gradually and finally becomes quite flattened. A maximum *Q* factor is reached at when the gap dimension reaches to the wavelength of the resonance mode. However, the resonant energy in the resonator is extremely weak at this gap distance as shown in Fig. 3. The limit *Q* value is over 10^3 for the 2μm-in-diameter microcavity. The FWHM is the bandwidth of a resonance mode. It is inversely proportional to the *Q* factor.

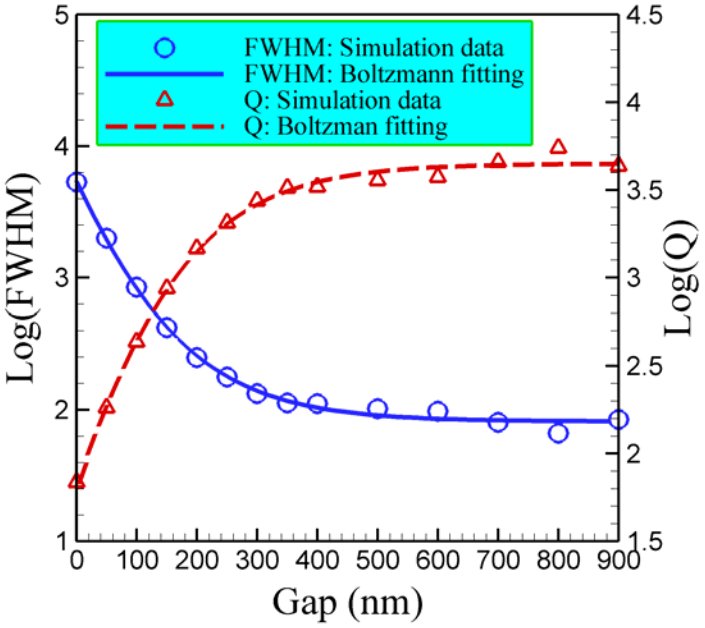

Figure 4. Gap effects on the Full Width at Half Maximum (FWHM) of the resonance band and the *Q* factor.

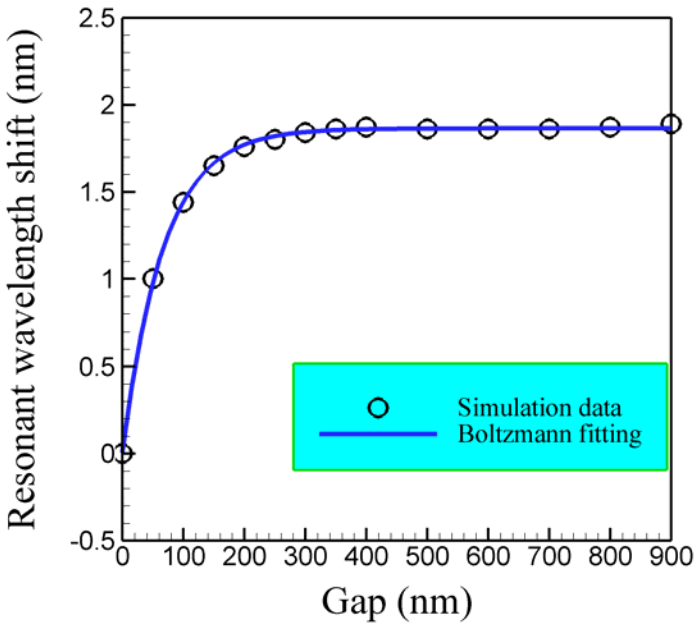

Figure 5. Gap variation vs. resonance frequency shift.

It is easy to understand the reduction of coupling efficiency at gap dimensions larger than the optimal value, because it is well-known that the evanescent field strength from a surface decays exponentially as a function of the distance to the surface. The longer the distance, the weaker is the strength. The evanescent field is almost negligible at a distance over one optical wavelength involved. How can we understand the reduction of the coupling efficiency for gaps smaller than the optimal gap? From the viewpoint of the evanescent strength, a smaller gap has a stronger strength and closer overlapping of the two evanescent fields from the resonator and the waveguide, respectively. A smaller gap affords more opportunities to photon tunneling. Indeed because of the enhanced photon tunneling, photons confined in the resonator tunnel back to the waveguide. As a result, a narrower gap reduces the coupling efficiency as a system. Therefore, an optimal gap for energy coupling exists as a trade-off between bidirectional coupling efficiencies.

Figure 5 shows the resonance wavelength shift against the gap variation. The shift is defined as $\lambda_g - \lambda_0$, where λ_0 is the resonance central wavelength under in-contact condition (zero gap) and λ_g is the resonance central wavelength corresponding to a gap. It is seen that with increasing gap the resonance wavelength shifts upward. The shift could be very appreciable (maximum is around 1.85 nm). However, the results indicate that the frequency

shifts reach to a stable and constant value after the gap distance increases to over 250nm. This implies that the gap dimension after a threshold value will not influence the resonance frequency. This trait is of great significance for applications using frequency shift characteristic such as in biosensors.[6,10]

Simultaneously considering Figs. 3 to 5, we suggest a trade-off among the coupling efficiency, the *Q* factor, and the stable resonance frequency requirement. For many sensor-based applications, it is feasible to sacrifice somewhat of the *Q* factor to guarantee the measurement of sensitive signals. A gap dimension after the optimal gap and at half of the maximum coupling efficiency can be chosen as the optimum gap in which both the *Q* factor and coupling efficiency are high, and the resonance frequency is not affected by a small variation in the gap dimension. This optimum gap concept is shown in Fig. 6 and this can be used as the guidance in the design of optical microcavity devices.

IV. Conclusion

Energy coupling and whispering-gallery mode optical resonances were simulated using the finite element solution of Maxwell's equations. It was found that the optical microcavities have a very strong energy storing property under optical resonance. The majority energy stores in a thin ring close to the periphery of the microcavity. An optimal gap dimension was found for maximum energy coupling from the waveguide to the resonant cavity. With increasing gap, the *Q* factor increases; while the FWHM decreases. The *Q* factor increases exponentially at the beginning before the gap reaches to the optimal gap for coupling; after passing the optimal gap, the increase of the *Q* factor slows down; and when the gap approaches to the optical wavelength the *Q* factor reaches to a limit maximum value. For very small gap, the resonance central frequency is strongly affected by the gap dimension variation. With increasing gap to over 250nm, the gap variation does not obviously affect the resonance frequency. An optimum gap can then be suggested at half maximum energy coupling where both the *Q* factor and coupling efficiency are high and the resonance frequency is stable.

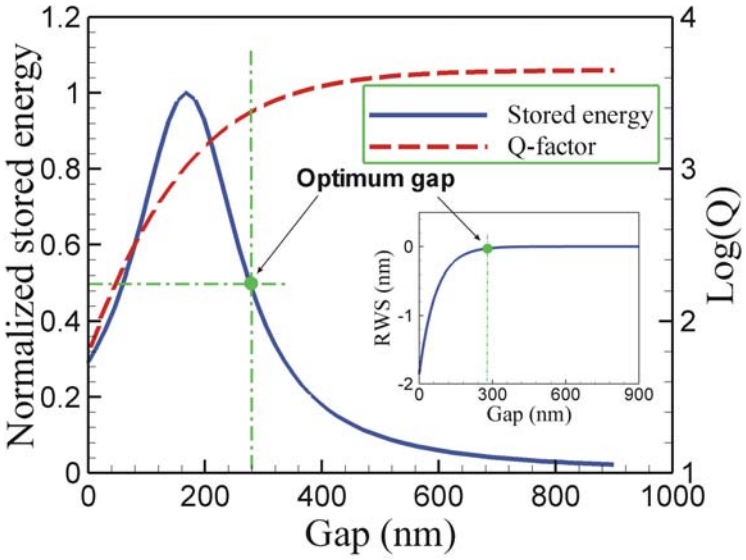

Figure 6. Introduction of the optimum gap concept.

Acknowledgments

Z. Guo is grateful to the support of the Academic Excellence Fund Awards (2003-2004, and 2005-2006) from Rutgers University and a grant from the National Science Foundation (CTS- 0541585) to the project.

References

[1]Hill, S. C., and Benner, R. E., "Morphology-Dependent Resonances," *Optical Effects Associated with Small Particles*, edited by P. W. Barber and P. K. Chang, World Scientific, Singapore, 1988, pp. 3-61.

[2]Vahala, K. J., "Optical Microcavities", *Nature*, Vol. 424, 2003, pp. 839, 846.

[3]Cai, M., Painter, Q., Vahala, K. J., and Sercel, P. C., "Fiber-Coupled Microsphere Laser", *Opt. Lett.*, Vol. 25, 2000,, pp. 1430, 1432.

[4]Little, B. E., Chu, S. T., Haus, H. A. Foresi, J., and Laine, J. P., "Microring Resonator Channel Dropping Filters", *J. Lightwave Tech.,* Vol. 15, 1997, pp. 998, 1005.

[5]Blom, F. C., van Dijk, D. R., Hoekstra, H. J., Driessen, A., and Popma, T. J. A., "Experimental Study of Integrated-Optics Micro-Cavity Resonators: Toward an All-Optical Switching Device," *Appl. Phys. Lett.,* Vol. 71, 1997, pp. 747, 749.

[6]Arnold, S., Khoshsima, M., Teraoka, I., and Vollmer, F., "Shift of Whispering-Gallery Modes in Microspheres by Protein Adsorption", *Opt. Lett.*, Vol. 28, 2003, pp. 272, 274.

[7]Schiller, S., and Byer, R. L., "High-Resolution Spectroscope of Whispering Gallery Modes in Large Dielectric Spheres," *Opt. Lett.,* Vol. 16, 1991, pp. 1138, 1140.

[8]Collot, L., Lefèvre-Seguin, V., Brune, M., Raimond, J. M., and Haroche, S., "Very High-Q Whispering Gallery Modes Resonances Observed on Fused Silica Microspheres," *Europhys. Lett*., Vol. 23, 1993, pp. 327, 333.

[9]Gorodetsky, M. L., Savchenkov, A. A., and Ilchenko, V. S., "Ultimate Q of Optical Microsphere Resonators," *Opt. Lett.,* Vol. 21, 1996, pp. 453, 455.

[10]Quan, H., and Guo, Z., "Simulation of Whispering-Gallery-Mode Resonance Shifts for Optical Miniature Biosensors," *J. Quantitative Spectroscopy & Radiative Transfer,* Vol. 93, 2005, pp. 231, 243.

[11]Gorodetsky, M. L., and Ilchenko, V. S., "Optical Microsphere Resonators: Optimal Coupling to High-Q Whispering-Gallery Modes," *J. Opt. Soc. Am. B,* Vol. 16, 1999, pp. 147, 154.

[12]Serpenguzel, A., Arnold, S., and Griffel, G., "Excitation of Resonances of Microspheres on an Optical Fiber", *Opt. Lett*., Vol. 20, 1995, pp. 654, 656.

[13]Knight, J. C., Cheung, G., Jacques, F., and Birks, T. A., "Phase-Matched Excitation of Whispering Gallery Mode Resonances Using a Fiber Taper," *Opt. Lett*., Vol. 22, 1997, pp. 1129, 1131.

[14]Quan, H., Guo, Z., Xu, L., and Pau, S., "Design, Fabrication and Characterization of Whispering-Gallery Mode Miniature Sensors", *Nanofabrication: Technologies, Devices, and Applications*, edited by W. Y. Lai, S. Pau, and O. D. López, Proceedings of SPIE Vol. 5592, SPIE, Bellingham, WA, 2005, pp. 373-381.

[15]Guo, Z., Quan, H., and Pau, S., "Optical Resonance in Fabricated Whispering-Gallery Mode Microcavity," *J. Heat Transfer,* Vol. 127, 2005, p. 808.

[16]Bohren, C. F., and Huffman, D. R., *Absorption and Scattering of Light by Small Particles*, John Wiley and Sons, New York, 1983.

[17]Chen, G., "Wave Effects on Radiative Transfer in Absorbing and Emitting Thin-Film Media", *Microscale Thermophysical Eng.* Vol. 1, 1997, pp. 215, 224.

[18]Siegel, R., and Howell ,J.R., *Thermal Radiation Heat Transfer*, 4th ed., Taylor & Francis, New York, 2001.

[19]Modest, M. F., *Radiative Heat Transfer,* 2nd ed., Academic Press, New York. 2003.

[20]Kumar, S., "Thermal Radiation Transport in Micro-Structures", *Thermal Science and Engr.* Vol. 2, 1992, pp. 149, 157.

[21]Tien, C. L., Majumdar, A., and Gerner, F. M., *Microscale Energy Transport*, Taylor & Francis, Washington, DC, 1997.

[22]Chen, G., "Heat Transfer in Micro- and Nanoscale Photonic Devices," *Annual Review of Heat Transfer*, edited by C.L. Tien, Vol. VII, 1996, pp. 1, 57.

[23]Grigoropoulos, C. P., Moon, S., Lee, M., Hatano, M., and Suzuki, K., "Thermal Transport in Melting and Recrystallization of Amorphous and Polycrystalline Si Thin Films," *Applied Physics A,* Vol. 69 (supplement), 1999, pp. S295, S298.

[24]Zhang, Z. M., and Fu, C. J., "Unusual Photon Tunneling in the Presence of a Layer with a Negative Refractive Index", *Applied Physics Letters,* Vol. 80 , 2002, pp. 1097,1099.

[25]Majumdar, A., "Thermoelectricity in Semiconductor Nanostructures," *Science,* Vol. 303, 2004, pp. 777, 778.

[26]Hagness, S. C., Rafizadeh, D., Ho, S. T., and Taflove, A., " FDTD Microcavity Simulations: Design and Experimental Realization of Waveguide-Coupled Single-Mode Ring and Whispering-Gallery-Mode Disk Resonators," *J. Lightware Tech.,* Vol. 15, 1997, pp. 2154, 2165.

[27]Silvester, P. P., "Finite Element Solution of Homogeneous Waveguide Problems", *Alta Frequenza,* Vol. 38, 1969, pp. 313, 317.